

## Transient Microneedle Insertion Into Hippocampus Triggers Neurogenesis and Decreases Amyloid Burden in a Mouse Model of Alzheimer's Disease

Shijie Song,\*†‡ Xiaoyung Kong,\*‡ Vasyl Sava,† Chuanhai Cao,§ Sandra Acosta,‡  
Cesar Borlongan,‡ and Juan Sanchez-Ramos\*†

\*James Haley VA Medical Center, Tampa, FL, USA

†Department of Neurology, Morsani College of Medicine, University of South Florida, Tampa, FL, USA

‡Department of Neurosurgery, Morsani College of Medicine, University of South Florida, Tampa, FL, USA

§Byrd Alzheimer's Institute, University of South Florida, Tampa, FL, USA

Targeted microlesions of the hippocampus have been reported to enhance neurogenesis in the subgranular zone (SGZ). The potential therapeutic impact of transient insertion of a microneedle was investigated in a mouse model of Alzheimer's disease (AD). We tested the hypothesis that transient microinjury to the brain elicits cellular responses that mediate beneficial regenerative processes. Brief stereotaxic insertion and removal of a microneedle into the right hippocampus of 14-month-old APP/PS1 mouse brains resulted in (a) stimulation of hippocampal neurogenesis and (b) reduction of amyloid- $\beta$  plaque number in the CA-1 region. This treatment also resulted in a trend toward improved performance in the radial arm water maze (RAWM). Further studies of fundamental cellular mechanisms of the brain's response to microinjury will be useful for investigation of potential neuroprotective and deleterious effects of targeted microlesions and deep brain stimulation in AD.

**Key words:** Neurogenesis; Transgenic APP/PS1 mice; Microneedle stimulation; Alzheimer's Disease (AD); Amyloid- $\beta$  (A $\beta$ )

### INTRODUCTION

Alzheimer's disease (AD) is an irreversible, progressive brain disorder that slowly diminishes memory and thinking skills, and eventually results in the inability to carry out simplest tasks. The underlying neuropathology is believed to begin at least a decade before memory and other cognitive problems appear<sup>1</sup>. During this prodromal stage, individuals appear to be symptom free, but significant changes are taking place in the brain. Abnormal deposits of proteins accumulate in extracellular amyloid plaques and tau tangles within neurons throughout the brain. The neurons become dysfunctional, lose synaptic connections with other neurons, and ultimately undergo cell death. The damage initially appears to take place in the hippocampus, an important node in the neural network that forms memories. As more neurons die, additional parts of the brain are affected, and brain atrophy occurs. By the final stage of Alzheimer's, damage is widespread, and brain tissue has shrunk significantly.

Microneedle stimulation (acupuncture) has been used to relieve pain in China for millennia. Many diseases of the central nervous system (CNS) could not be treated by this method because of inaccessibility of the brain to a microneedle. In the last decade, deep brain stimulation (DBS) through chronically implanted metal electrodes into specific brain regions has become a common therapeutic choice for refractory movement disorders such as Parkinson's disease (PD), tremors, and dystonia (reviewed in<sup>2–4</sup>). More recently, DBS has been applied to psychiatric and behavioral disorders including depression, obsessive-compulsive disorder (OCD), addiction, and, most recently, for disorders of consciousness<sup>5–10</sup>. Long-term implantation of a fine metal electrode, even without chronic electrical stimulation, may produce unwanted effects, such as mild to severe inflammatory responses, microhemorrhages, and infections<sup>11</sup>. Neuropathological examination of brain tissue from patients with DBS revealed activated astrocytes and microglia regardless of the underlying

Received November 10, 2015; final acceptance May 18, 2016. Online prepub date: February 18, 2016.

Address correspondence to Juan Sanchez-Ramos, Ph.D., M.D., Department of Neurology, Morsani College of Medicine, University of South Florida, 13220 Laurel Drive (FOB), Tampa, FL 33612, USA. Tel: (813) 974-5841; Fax: (813) 974-8032; E-mail: [jsramos@health.usf.edu](mailto:jsramos@health.usf.edu) or Shijie Song, M.D., Department of Neurology, Morsani College of Medicine, University of South Florida, 13220 Laurel Drive (FOB), Tampa, FL 33612, USA. E-mail: [ssong@health.usf.edu](mailto:ssong@health.usf.edu)

disease<sup>12–17</sup>. Electrical stimulation is not required to see signs of neuroinflammation; inflammatory changes have been observed around recording electrodes used for characterizing epileptogenic tissue and around cerebral spinal fluid (CSF) shunt catheters<sup>11,18</sup>. Earlier studies of “stab injuries,” in which a foreign object (usually a metal) was inserted into rodent brain and immediately removed, had pointed to the importance of chemokine expression in mediating microgliosis and astrocytosis<sup>19–22</sup>. The acute and subacute reactions to transient implantation of a metal microneedle in the hippocampus were recently reported<sup>23</sup>. The needle insertion triggered a robust cellular response characterized by proliferation of microglia and astrocytes and resulted in stimulation of neurogenesis in the subgranular zone (SGZ) of the hippocampus.

The primary objective of the present study was to determine whether brief microneedle stimulation would increase hippocampal neurogenesis in a transgenic mouse model of AD (Tg APP/PS1) and improve performance on a hippocampal-dependent learning task, such as radial arm water maze (RAWM). A secondary objective was to determine if the needle insertion might activate cellular mechanisms to improve clearance of the amyloid- $\beta$  (A $\beta$ ) deposits in a transgenic mouse model of AD (Tg APP/PS1).

## MATERIALS AND METHODS

All procedures described here were reviewed and approved by the institutional animal care and use committee (IACUC) of the University of South Florida and the James A. Haley VA Research Service.

### *Animals*

C57BL/6 male mice (8–10 weeks old,  $n = 6$ ) were purchased from Harlan Laboratories (Indianapolis, IN, USA). Transgenic (Tg) green fluorescent protein (GFP) male mice [ $n = 6$ , C57BL/6-Tg (ACTB-EGFP) 10sb/J, 003291] and Tg APP/PS1 male mice ( $n = 12$ ) were purchased from Jackson Laboratory (Bar Harbor, ME, USA) and were aged to 14 months before euthanasia.

### *Bone Marrow Harvest and Generation of Chimeric Mice That Harbor GFP-Expressing (GFP<sup>+</sup>) Bone Marrow Cells*

The procedure for bone marrow harvesting from Tg GFP<sup>+</sup> mice has been previously published by Sanchez-Ramos and colleagues<sup>24,25</sup>. Briefly, bone marrow cells were collected from femurs and tibias of adult male Tg GFP<sup>+</sup> mice by flushing the bone shaft with phosphate-buffered saline (PBS) + 0.5% bovine serum albumin (BSA) + 2 mM ethylenediaminetetraacetic acid (EDTA) (all from Sigma-Aldrich, St. Louis, MO, USA).

To generate chimeric mice, Tg APP/PS1 mice (aged 3 months) were lethally irradiated with 8 gray (Gy) total body irradiation (delivered in two fractions of 4 Gy at

an interval of 4 h) at a dose rate of 1.03 Gy/min in a Gammacell 40 Exactor (Best Theratronics Ltd., Kanata, ON, Canada)<sup>26</sup>. Following irradiation, the mice were transplanted with  $10 \times 10^6$  bone marrow-derived mononuclear cells (BM-MNCs) from Tg GFP<sup>+</sup> mice infused via tail vein. Bone marrow-derived cells in the rescued mice were readily tracked by virtue of their green fluorescence. Examination of blood smears from tail clippings for the presence of green monocytes confirmed successful engraftment. An average of 95–100% of the irradiated mice had successful engraftment and exhibited GFP<sup>+</sup> mononuclear cells in their peripheral blood<sup>27</sup>.

### *Stereotaxic Insertion and Removal of Microneedle*

Animals were anesthetized with ketamine [100 mg/kg, intraperitoneally (IP); Putney Inc., Portland, ME, USA] and xylazine (10 mg/kg, IP; Bayer Animal Health, Shawnee Mission, KS, USA) and placed into a stereotaxic frame. Using the bregma as the reference point, a trephine hole was then drilled into the skull, and the needle was gently inserted into the hippocampus [anterior–posterior (AP), 2.5 mm; medial–lateral (ML), 1.3 mm; dorsal–ventral (DV), 3.5mm] and slowly removed. The total time for insertion and removal of the microneedle was 15 s. Mice also received 5-bromo-2'-deoxyuridine (BrdU) (Sigma-Aldrich) by IP injections (100 mg/kg twice per day, for 3 days) to label nascent cells starting on the day of transient insertion of the needle.

### *RAWM Test*

The RAWM is a task designed to test spatial learning and memory and was originally developed to test animals' ability to navigate to a specific location (place learning); however, it can easily be adapted to test spatial working memory. This task is hippocampal dependent and highly sensitive to hippocampal functional integrity, although other brain structures, such as the prefrontal cortex and basal forebrain, are important. The RAWM was administered at baseline (before stereotaxic surgery) and 7 weeks after microneedle insertion and removal. For baseline performance, mice were tested for 4 consecutive days in the RAWM task, and then the Tg mice were divided into two groups: one received a transient insertion of a microneedle to the dorsum of the hippocampus, and the other mice underwent sham surgery (no penetration of calvarium). Four weeks after microneedle stimulation (or sham surgery), all mice were retested in the RAWM for 4 consecutive days. For RAWM testing, an aluminum insert was introduced into a 100-cm pool in order to divide the pool into six equally spaced swim arms (30.5-cm length, 19-cm width) radiating from a central circular swim area (40-cm diameter). The insert extended 5 cm above the surface of the water, allowing the mice to easily view surrounding visual cues, which were generously placed outside of the

pool. Visual/spatial cues consisted of large brightly colored two-dimensional (2D) and 3D objects, including a beach ball, poster, and inflatable pool toys. During testing, the pool water was maintained at 23–27°C. In one of the arms, a transparent 9-cm submerged escape platform was placed 1.5 cm below the water near the wall end. Each mouse was given five 1-min trials per day. The last of the four consecutive acquisition trials [trial 4 (T4)] and a 30-min delayed retention trial (T5) are indices of working memory. On any given day, the escape platform location was placed at the end of one of the six arms, with the platform moved to a different arm in a semirandom fashion for each day of testing. In contrast to the stationary platform of the Morris water maze, moving the escape platform forced the animal to learn a new platform location daily, thereby evaluating working memory. On each day, different start arms for each of the five daily trials were selected from the remaining five swim arms in a semirandom sequence that involved all five arms. For any given trial, the mouse was placed into that trial's start arm, facing the center swim area, and given 60 s to find the platform. When the mouse made an incorrect choice, it was gently pulled back to that trial's start arm and an error was recorded. An error was also recorded if the mouse failed to make a choice in 20 s (in which case it was returned to that trial's start arm), or if the animal entered the platform-containing arm but failed to locate the platform. A 30-s stay was given once the mouse had found the platform. If the mouse did not find the platform within a 60-s trial, it was guided by the experimenter to the platform, allowed to stay for 30 s, and was assigned a latency of 60 s. Both errors (incorrect arm choices) and escape latency were recorded for each daily trial.

#### *Tissue Preparation and Sectioning*

Six mice from each group [nontransgenic (NT) controls, 14-month-old Tg APP/PS1 mice treated with micro-needle, and 14-month-old Tg APP/PS1 mice that had sham surgery] underwent histological analyses to determine the extent of neurogenesis in the hippocampus and A $\beta$  reduction. After completion of the RAWM, 7 weeks after needle stimulation, mice were anesthetized with 10% chloral hydrate (Sigma-Aldrich) and a transcardiac perfusion of the brain with 20 ml of saline and 50 ml of 4% paraformaldehyde (PFA; Sigma-Aldrich) was done. The brain was removed and fixed for 48 h in the same solution. After fixing, the brains were immersed overnight in 25% sucrose + 4% PFA in PBS (Sigma-Aldrich). Thirty-micrometer-thick frozen sections through the hippocampus were prepared and stored in vials containing a cryopreservation solution.

#### *Immunohistochemistry*

Selective immunostaining of astrocytes and microglia was performed with antibodies to glial fibrillary acidic

protein (GFAP) and ionized calcium-binding adapter molecule-1 (Iba1), respectively. Iba1 is a protein that is specifically expressed in macrophages/microglia and is upregulated during the activation of these cells. Antibodies to doublecortin (DCX) were used to label newborn neurons in the dentate gyrus (DG) of the hippocampus. Brain sections were preincubated in PBS containing 10% normal serum (goat or donkey; Vector Laboratories Inc., Burlingame, CA, USA) and 0.3% Triton X-100 (Sigma Labs Inc., Santa Fe, NM, USA) for 30 min. The sections were then transferred to a solution containing primary antibodies in 1% normal serum, 0.3% Triton X-100/PBS, and incubated overnight at 4°C. The specific antibodies used in each experiment were as follows: rabbit anti-Iba1 (Wako Chemicals USA Inc., Richmond, VA, USA), 1:500; rabbit anti-GFAP (BioGenex Laboratories Inc., San Ramon, CA, USA) 1:50 in PBS; rabbit anti-DCX (Abcam, Burlingame, CA, USA), 1:1,000 containing 1:100 normal serum without Triton X-100. After incubation with primary antibody, the sections were washed and incubated for 1 h with Alexa Fluor 488 goat anti-rabbit immunoglobulin G (IgG) diluted 1:400 in PBS (Invitrogen, Grand Island, NY, USA) at room temperature. The sections were then rinsed in PBS three times and covered with a cover glass. Green fluorescence signals from the labeled cells were visualized with fluorescence microscopy using appropriate filters.

#### *Quantitative Image Analysis of Amyloid Burden*

Images were acquired at a magnification of 200 $\times$  as digitized tagged-image format files (TIFF) to retain maximum resolution using an Olympus BX60 microscope with an attached digital camera system (DP-70; Olympus, Tokyo, Japan). Images of six 30- $\mu$ m-thick sections (180  $\mu$ m apart) from each mouse were captured from serially sectioned hippocampi on both the left and right sides. Using ImageJ software [National Institutes of Health (NIH), Bethesda, MD, USA], the red channel (for the amyloid stain) was selected and converted into a monochrome signal. Then a threshold optical density was obtained that discriminated staining from background. The thresholded signal was quantified as percent of the visual field for each image. Data were reported as the percentage of labeled area captured (positive pixels) divided by the full area captured (total pixels). The fluorescence signals from each mouse hippocampus (separate analyses for each side) were averaged and used to calculate the mean signal (% of the visual field) for each group of mice.

As a surrogate index of neurogenesis, the expression of DCX, a marker of immature neurons<sup>28</sup>, was measured in the DG of hippocampi using the approach described above. Bias was eliminated by using a blinded examiner who analyzed the region of interest (ROI) represented by the sampling of six sections per mouse DG on the right

side and six sections on the left side. Each analysis was done by a single examiner blinded to sample identities. In addition to semiautomatically measuring DCX signal (as described above for the amyloid measurements), an unbiased estimate of the number of DCX<sup>+</sup> cells in the DG was performed on coded sections as previously described<sup>29,30</sup>. Briefly, double-labeled cells (BrdU<sup>+</sup> cells that coexpressed DCX) were counted in every sixth section (each section separated by 180  $\mu$ m) using a modification to the optical dissector method; cells on the upper and lower planes were not counted to avoid counting partial cells. Resulting numbers were tallied and multiplied by tissue thickness (30  $\mu$ m) and the number of intervening sections.

### Data Analysis

A summary of RAWM data was prepared by determining the mean error score for trials 1, 4, and 5. The RAWM data were analyzed using both two-way repeated-measures analysis of variance (ANOVA) and one-way ANOVAs. *t*-Tests comparing treatment groups against NT controls in trial 5 were run followed by a correction for multiple comparisons (Sidak's multiple comparisons test). Analysis of histological data comparing the lesioned side to the unlesioned side utilized unpaired *t*-tests with equal variances (GraphPad Prism version 6.00 for Mac OS, GraphPad Software, La Jolla, CA, USA).

## RESULTS

The RAWM was administered at baseline (before stereotaxic surgery) and 7 weeks after brief stereotaxic insertion and removal of a microneedle that targeted dorsal hippocampi on the right side of the brain. The microlesioned Tg APP/PS1 mice exhibited a 38.8% reduction in errors compared to the nonlesioned Tg APP/PS1 mice on the delayed memory retention trial (trial 5) (Fig. 1C). Two-way ANOVA of the data showed that trial number, but not treatment (lesion vs. no lesion), contributed significantly to total variation. One-way analysis of trial 5 data followed by *t*-tests with correction for multiple comparisons showed that both lesioned and nonlesioned Tg animals were significantly different than the NT lesioned mice. Although the data suggested an improved performance by the lesioned Tg mice compared to the nonlesioned Tg mice (Fig. 1C), these results did not reach statistical significance.

Seven weeks after the surgery and after the last RAWM test, the animals were euthanized and amyloid burden was determined (Fig. 2). Simple insertion and removal of the needle triggered a repair response in which the A $\beta$  signal was reduced over a period of 7 weeks by greater than 50% in the CA-1 region. In addition, the GFP<sup>+</sup> cells around and within amyloid plaques were increased greater than twofold (Fig. 2D). These mice had been transplanted with

GFP<sup>+</sup> bone marrow at 3 months of age. Hence, the GFP<sup>+</sup> cells that decorate the A $\beta$  plaques are derived from circulating GFP<sup>+</sup> blood cells. Many GFP<sup>+</sup> cells coexpress Iba1, indicating these cells have differentiated into microglia (data not shown). The recruitment of GFP<sup>+</sup> bone marrow cells to the site of the lesion and their differentiation into Iba1<sup>+</sup> microglia have been reported in an earlier microlesion study in normal mice<sup>23</sup>. Moreover, the microlesion resulted in increased hippocampal astrogliosis (GFAP signal data not shown) as reported in the earlier study.

In addition to decreased amyloid burden the microlesion promoted hippocampal neurogenesis (Fig. 3). The DCX signal, a marker of immature neurons in the SGZ, was significantly increased by the microneedle stimulation of the right dorsal hippocampus compared to the untreated side. Estimates of numbers of newborn neurons (numbers of DCX cells that were labeled at birth with BrdU) confirmed a significant increase of double-labeled DCX/BrdU<sup>+</sup> cells triggered by the focal microlesion in Tg AD mice.

## DISCUSSION

Focal microlesions of the hippocampus produced by transient insertion and removal of a microneedle in a transgenic mouse model of AD was effective in decreasing amyloid burden and increasing neurogenesis. Similar results on reduction of amyloid burden and promotion of hippocampal neurogenesis in Tg AD mice have been observed following a course of granulocyte colony-stimulating factor (G-CSF) treatment in the same transgenic mouse model of AD<sup>27</sup>. Following a course of G-CSF treatment of both young and old Tg APP/PS1 mice, the therapeutic effect on amyloid reduction was associated with improved performance in the RAWM, similar to the effects of microlesioning of the hippocampus reported here. More recently, microlesions of the hippocampus in young C57BL/6J mice were reported to promote hippocampal neurogenesis and to increase total microgliosis and astrogliosis<sup>23</sup>. In that microlesion study, a significant proportion of the microglia (26%) were derived from circulating monocytes. A cascade of cytokine and chemokine release appeared to play a role in recruitment of monocytes into the brain where they differentiated into microglia<sup>23</sup>. In the present study, there was no attempt to characterize the phenotype of the GFP<sup>+</sup> cells. However, on the basis of our earlier work, it is likely that GFP<sup>+</sup> cells decorating the amyloid plaques were recruited to the site of the lesion where they differentiated into microglia expressing Iba1<sup>23</sup>. It is assumed that increased macrophage activity of the newly recruited microglia promotes clearance of plaques. Interventions that decrease the amyloid burden have been demonstrated to improve performance in the RAWM in other studies using the same Tg APP/PS1 mouse model of AD<sup>27,31</sup>.



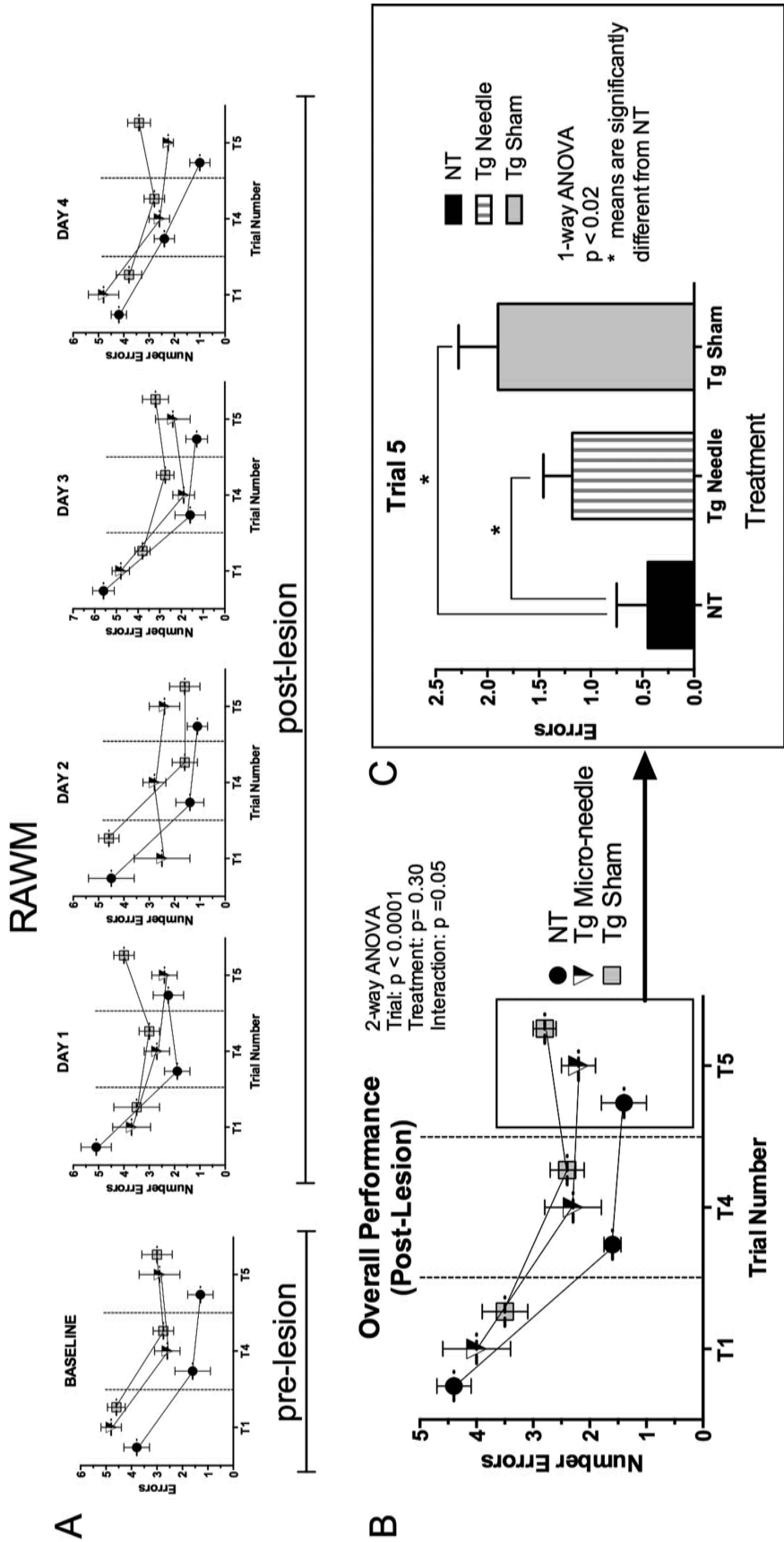


**Figure 1.** Transient microneedle insertion into the right hippocampus improved spatial memory impairment of Tg APP/PS1 mice (total  $n = 12$  mice; 6 mice in each experimental group) and nontransgenic (NT) mice ( $n = 6$ ). Data are plotted as mean number of errors on the y-axis and trials on the x-axis. (A) Number of errors plotted against trial number before the microlesion (BASELINE) and consecutive performances (days 1 to 4) exhibited 4 weeks after the lesions. (B) The overall performance (mean scores of the three groups of animals) at T1, T4, and T5. Two-way analysis of variance (ANOVA) revealed that trial number, but not treatment, contributed significantly to total variation. Reversal training data analysis was performed on trial 5. (C) Mean number of errors plotted against treatment on trial 5. One-way ANOVA followed by  $t$ -tests with multiple comparisons revealed that all means in trial 5 differed from the NT control ( $*p < 0.05$ ). The lesioned Tg mice exhibited a 37.8% reduction of errors in T5 than nonlesioned Tg mice, but the difference did not reach statistical significance.

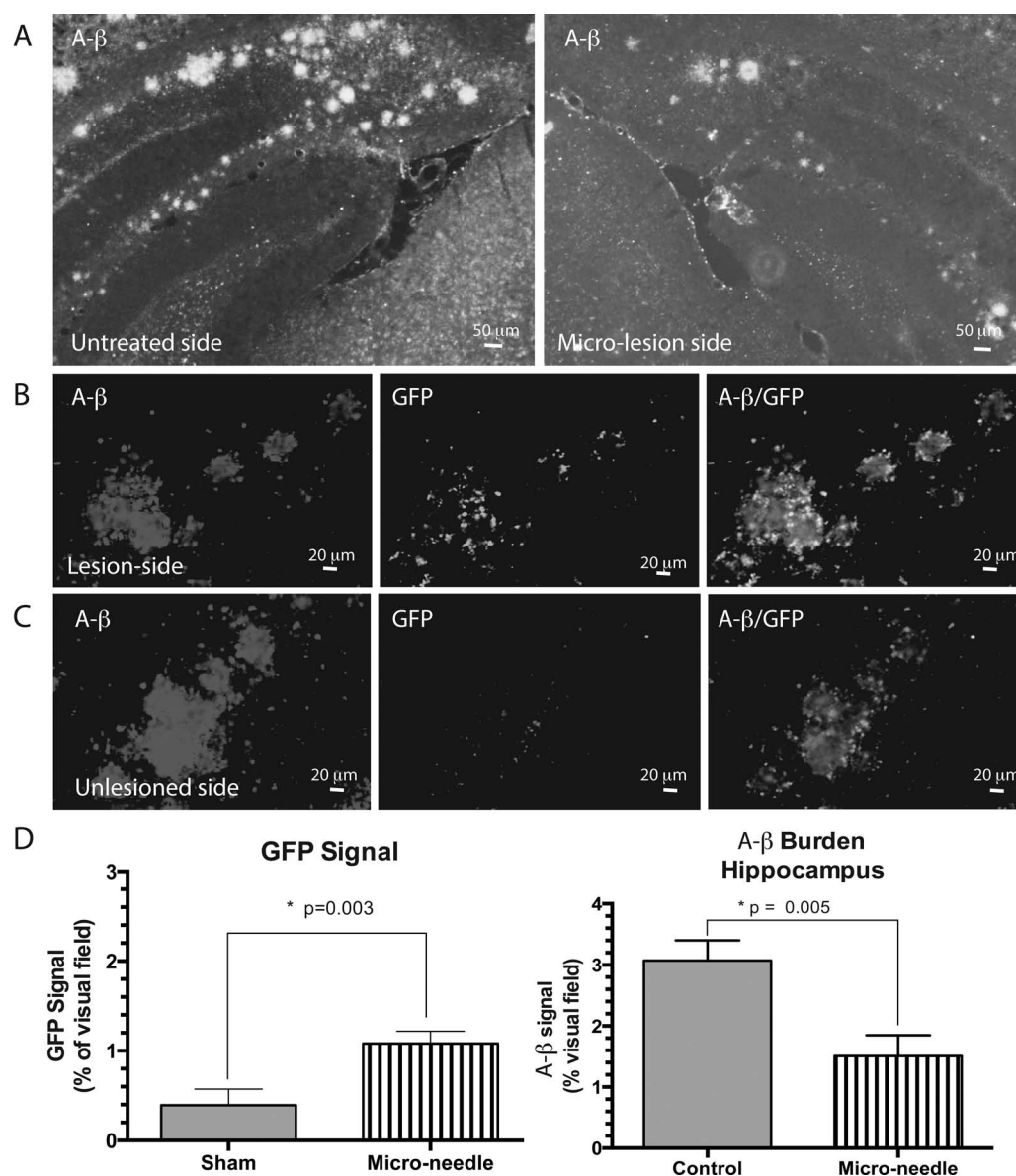


**Figure 2.** Effect of microlesioning on amyloid burden in CA-1 of hippocampi. Seven weeks after transient insertion of the micro-needle, animals were euthanized, and sections through the hippocampus were processed for amyloid- $\beta$  (A $\beta$ ) immunoreactivity and determination of A $\beta$  burden. (A) Left: Untreated hippocampi of Tg APP/PS1 mice. Abundant A $\beta$  plaques are seen in the hippocampus, especially the CA-1 region. Right: Reduction of A $\beta$  plaques (scale bars: 50  $\mu$ m). (B) Left: Increased magnification of the plaques on the lesioned side (scale bars: 20  $\mu$ m). Middle: GFP $^{+}$  signal in the same section. Right: Merged image of the hippocampal section (A $\beta$ /GFP $^{+}$ ). (C) Left: Increased magnification of the plaques on the unlesioned control side (scale bars: 20  $\mu$ m). Middle: GFP $^{+}$  signal in the same section. Right: Merged image of the hippocampal section (A $\beta$ /GFP $^{+}$ ). (D) Summary data (mean amyloid burden per experimental cohort, with  $n = 6$  mice in each group). Graph on the right shows a significant amyloid burden reduction in hippocampus. Graph on the left shows an increase in GFP signal, indicating a recruitment of GFP $^{+}$  cells from the peripheral circulation in these chimeric Tg mice.

In light of the observations that microlesions of the hippocampus stimulated neurogenesis in normal young mice, it was interesting to observe a similar cellular response (i.e., neurogenesis) would still occur in old Tg AD mice. Unexpectedly, the unilateral focal microlesion also resulted in (a) decreased amyloid burden and (b) a positive impact

on spatial memory. The Tg AD mice that were lesioned performed better than Tg AD mice that underwent sham surgery. The lesioned group of Tg AD mice committed 38% less errors than nonlesioned Tg AD mice when tested after the reversal training, but this improvement did not reach statistical significance. The number of animals per

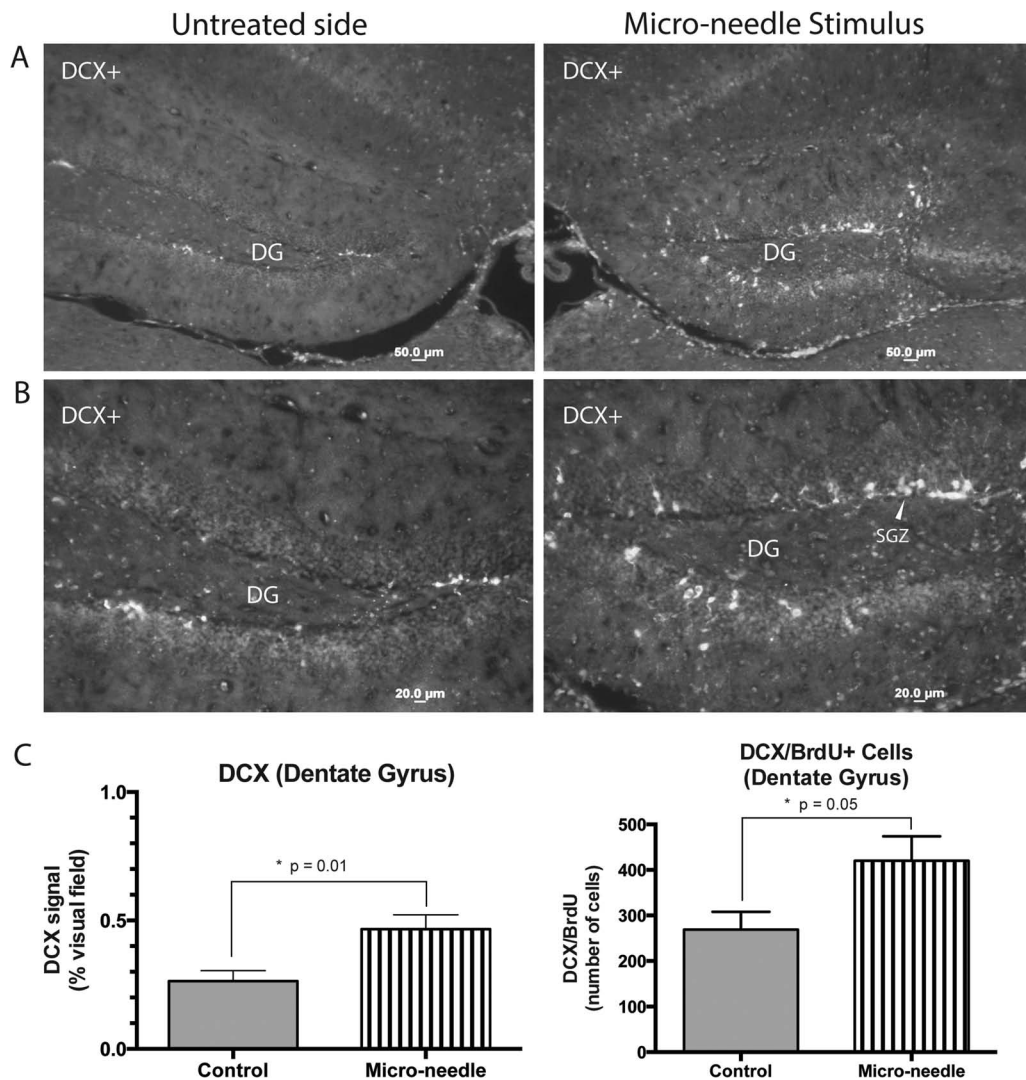


**Figure 3.** Sterile acupuncture needle (200  $\mu$ m maximum shaft diameter) was transiently inserted stereotactically into the dorsal hippocampi of 14-month-old chimeric Tg APP/PS1 mice or NT mice that had received bone marrow-derived mononuclear cell (BM-MNC) transplantation with GFP<sup>+</sup> bone marrow cells at age 3 months. Mice were injected with 5-bromo-2'-deoxyuridine (BrdU) (100 mg/kg, IP, twice a day for 3 days) to label newly formed cells, followed by microneedle insertion. Animals were euthanized after completion of RAWM, 7 weeks after placement of the focal microlesion. (A) DCX<sup>+</sup> cells in the subgranular zone (SGZ). Left: Control side (no lesion placement). Right: Increased expression of DCX<sup>+</sup> cells in the SGZ (the lesioned side). Scale bars: 50  $\mu$ m. (B) Same sections at higher magnification (scale bars: 20  $\mu$ m). (C) The bar graphs indicate a significantly higher expression of GFP<sup>+</sup> signal in the microlesioned hippocampus compared to the unlesioned control side. The graph on the right shows the number of newborn neurons (double-labeled DCX/BrdU<sup>+</sup> cells) in the SGZ of the hippocampus was increased on the side of the lesion.

group was only six, and it is likely that a larger sample size might have revealed a statistically significant improvement in performance in the RAWM.

#### Clinical Significance

DBS through chronically implanted metal electrodes into specific brain regions is becoming a common therapeutic choice for refractory movement disorders such as PD, tremors, and dystonia. More recently, DBS has been applied to psychiatric and behavioral disorders including

depression, OCD, addiction, and, most recently, for disorders of consciousness<sup>5,8-10</sup>. The potential deleterious effects of short-term or long-term electrode implantation are well recognized. Examination of brain tissue from patients with DBS has revealed activated astrocytes and microglia regardless of the underlying disease. Electrical stimulation is not required to see signs of neuroinflammation; inflammatory changes have been observed around recording electrodes used for characterizing epileptogenic tissue and around CSF shunt catheters.

The increasing number of neurosurgical interventions to treat cognitive and psychiatric conditions calls for a closer look at mechanisms responsible for therapeutic benefits as attempted in the present study. Stimulation of the entorhinal cortex has been reported to promote adult neurogenesis and facilitate spatial memory in mice<sup>32</sup>. Memory enhancement was reported as a result of DBS of the entorhinal area of patients who were undergoing a workup for epilepsy surgery<sup>33</sup>. This approach was applied in a phase 1 study in patients with AD<sup>34</sup>. The investigators hypothesized that fornix/hypothalamus DBS could modulate neurophysiological activity in these pathological circuits and possibly produce clinical benefits. Continuous DBS for 12 months drove neural activity in the memory circuit, including the entorhinal and hippocampal areas. Evaluation of the AD Assessment Scale cognitive subscale and the Mini Mental State Examination suggested possible improvements and/or slowing in the rate of cognitive decline at 6 and 12 months in some patients<sup>34</sup>. There were no serious adverse events<sup>34</sup>.

The findings presented here, along with the previous reports of beneficial effects of DBS in AD patients, provide a strong impetus for further investigations of fundamental cellular mechanisms of the brain's response to microinjury in animal models. As the cellular and humoral mechanisms of microlesioning are better understood, it will be possible to develop novel surgical and pharmacological targets for intervention and treatment of neurocognitive disorders.

**ACKNOWLEDGMENTS:** *This study is supported by a VA Merit Grant to S. Song. The contents of this research article do not represent the views of the Department of Veterans Affairs or the US Government. S.S., V.S., and J.S.-R. have submitted a patent application on the use of microstimulation to trigger neurogenesis.*

## REFERENCES

1. Sperling RA, Aisen PS, Beckett LA, Bennett DA, Craft S, Fagan AM, Iwatsubo T, Jack CR Jr, Kaye J, Montine TJ, Park DC, Reiman EM, Rowe CC, Siemers E, Stern Y, Yaffe K, Carrillo MC, Thies B, Morrison-Bogorad M, Wagster MV, Phelps CH. Toward defining the preclinical stages of Alzheimer's disease: Recommendations from the National Institute on Aging-Alzheimer's Association workgroups on diagnostic guidelines for Alzheimer's disease. *Alzheimers Dement*. 2011;7(3):280–92.
2. Bronstein JM, Tagliati M, Alterman RL, Lozano AM, Volkmann J, Stefani A, Horak FB, Okun MS, Foote KD, Krack P, Pahwa R, Henderson JM, Hariz MI, Bakay RA, Rezai A, Marks WJ Jr, Moro E, Vitek JL, Weaver FM, Gross RE, DeLong MR. Deep brain stimulation for Parkinson disease: An expert consensus and review of key issues. *Arch Neurol*. 2011;68(2):165.
3. Flora ED, Perera CL, Cameron AL, Maddern GJ. Deep brain stimulation for essential tremor: A systematic review. *Mov Disord*. 2010;25(11):1550–9.
4. Krack P, Vercueil L. Review of the functional surgical treatment of dystonia. *Eur J Neurol*. 2001;8(5):389–99.
5. de Koning PP, Figee M, van den Munckhof P, Schuurman PR, Denys D. Current status of deep brain stimulation for obsessive-compulsive disorder: A clinical review of different targets. *Curr Psychiatry Rep*. 2011;13(4):274–82.
6. Conca A, Di Pauli J, Hinterhuber H, Kapfhammer HP. [Deep brain stimulation: A review on current research]. *Neuropsychiatr*. 2011;25(1):1–8.
7. Luigjes J, van den Brink W, Feenstra M, van den Munckhof P, Schuurman PR, Schippers R, Mazaheri A, De Vries TJ, Denys D. Deep brain stimulation in addiction: A review of potential brain targets. *Mol Psychiatry*. 2012;17(6):572–83.
8. Marangell LB, Martinez M, Jurdi RA, Zboyan H. Neurostimulation therapies in depression: A review of new modalities. *Acta Psychiatr Scand*. 2007;116(3):174–81.
9. Sen AN, Campbell PG, Yadla S, Jallo J, Sharan AD. Deep brain stimulation in the management of disorders of consciousness: A review of physiology, previous reports, and ethical considerations. *Neurosurg Focus*. 2010;29(2):E14.
10. Shah SA, Schiff ND. Central thalamic deep brain stimulation for cognitive neuromodulation—a review of proposed mechanisms and investigational studies. *Eur J Neurosci*. 2010;32(7):1135–44.
11. Stephan CL, Kepes JJ, SantaCruz K, Wilkinson SB, Fegley B, Osorio I. Spectrum of clinical and histopathologic responses to intracranial electrodes: From multifocal aseptic meningitis to multifocal hypersensitivity-type meningo-vasculitis. *Epilepsia*. 2001;42(7):895–901.
12. Burbaud P, Vital A, Rougier A, Bouillot S, Guehl D, Cuny E, Ferrer X, Lagueny A, Bioulac B. Minimal tissue damage after stimulation of the motor thalamus in a case of chorea-acanthocytosis. *Neurology*. 2002;59(12):1982–4.
13. Chou KL, Forman MS, Trojanowski JQ, Hurtig HI, Baltuch GH. Subthalamic nucleus deep brain stimulation in a patient with levodopa-responsive multiple system atrophy. Case report. *J Neurosurg*. 2004;100(3):553–6.
14. Henderson JM. Vagal nerve stimulation versus deep brain stimulation for treatment-resistant depression: Show me the data. *Clin Neurosurg*. 2007;54:88–90.
15. Nielsen MS, Bjarkam CR, Sorensen JC, Bojsen-Moller M, Sunde NA, Ostergaard K. Chronic subthalamic high-frequency deep brain stimulation in Parkinson's disease—a histopathological study. *Eur J Neurol*. 2007;14(2):132–8.
16. Vedam-Mai V, van Battum EY, Kamphuis W, Feenstra MG, Denys D, Reynolds BA, Okun MS, Hol EM. Deep brain stimulation and the role of astrocytes. *Mol Psychiatry*. 2012;17(2):124–31, 115.
17. Vedam-Mai V, Yachnis A, Ullman M, Javedan SP, Okun MS. Postmortem observation of collagenous lead tip region fibrosis as a rare complication of DBS. *Mov Disord*. 2012;27(4):565–9.
18. Del Bigio MR. Biological reactions to cerebrospinal fluid shunt devices: A review of the cellular pathology. *Neurosurgery*. 1998;42(2):319–25; Discussion 325–6.
19. Glabinski AR, Balasingam V, Tani M, Kunkel SL, Strieter RM, Yong VW, Ransohoff RM. Chemokine monocyte chemoattractant protein-1 is expressed by astrocytes after mechanical injury to the brain. *J Immunol*. 1996;156(11):4363–8.
20. Ghirnikar RS, Lee YL, He TR, Eng LF. Chemokine expression in rat stab wound brain injury. *J Neurosci Res*. 1996;46(6):727–33.
21. Fujita T, Yoshimine T, Maruno M, Hayakawa T. Cellular dynamics of macrophages and microglial cells in reaction to



- stab wounds in rat cerebral cortex. *Acta Neurochir (Wien)* 1998;140(3):275–9.
22. Kaur C, Ling EA, Wong WC. Origin and fate of neural macrophages in a stab wound of the brain of the young rat. *J Anat.* 1987;154:215–27.
  23. Song S, Song S, Cao C, Lin X, Li K, Sava V, Sanchez-Ramos J. Hippocampal neurogenesis and the brain repair response to brief stereotaxic insertion of a microneedle. *Stem Cells Int.* 2013;2013:205878.
  24. Sanchez-Ramos J, Song S, Cardozo-Pelaez F, Hazzi C, Stedeford T, Willing A, Freeman TB, Saporta S, Janssen W, Patel N, Cooper DR, Sanberg PR. Adult bone marrow stromal cells differentiate into neural cells in vitro. *Exp Neurol.* 2000;164:247–56.
  25. Song S, Sanchez-Ramos J. Preparation of neural progenitors from bone marrow and umbilical cord blood. In: Zigova T, Sanberg PR, Sanchez-Ramos J, editors. *Protocols for neural stem cell methods*. Vol. 198. *Methods in molecular biology*. Totowa (NJ): Human Press; 2002. p. 79–88.
  26. Furuya T, Tanaka R, Urabe T, Hayakawa J, Migita M, Shimada T, Mizuno Y, Mochizuki H. Establishment of modified chimeric mice using GFP bone marrow as a model for neurological disorders. *Neuroreport* 2003;14(4): 629–31.
  27. Sanchez-Ramos J, Song S, Sava V, Catlow B, Lin X, Mori T, Cao C, Arendash GW. Granulocyte colony stimulating factor decreases brain amyloid burden and reverses cognitive impairment in Alzheimer's mice. *Neuroscience* 2009;163(1):55–72.
  28. von Bohlen und Halbach O. Immunohistological markers for staging neurogenesis in adult hippocampus. *Cell Tissue Res.* 2007;329(3):409–20.
  29. Shors TJ, Miesegaes G, Beylin A, Zhao M, Rydel T, Gould E. Neurogenesis in the adult is involved in the formation of trace memories. *Nature* 2001;410(6826):372–6.
  30. Catlow BJ, Song S, Paredes DA, Kirstein CL, Sanchez-Ramos J. Effects of psilocybin on hippocampal neurogenesis and extinction of trace fear conditioning. *Exp Brain Res.* 2013;228(4):481–91.
  31. Boyd TD, Bennett SP, Mori T, Governatori N, Runfeldt M, Norden M, Padmanabhan J, Neame P, Wefes I, Sanchez-Ramos J, Arendash GW, Potter H. GM-CSF upregulated in rheumatoid arthritis reverses cognitive impairment and amyloidosis in Alzheimer mice. *J Alzheimers Dis.* 2010; 21(2):507–18.
  32. Stone SS, Teixeira CM, Devito LM, Zaslavsky K, Josselyn SA, Lozano AM, Frankland PW. Stimulation of entorhinal cortex promotes adult neurogenesis and facilitates spatial memory. *J Neurosci.* 2011;31(38):13469–84.
  33. Suthana N, Haneef Z, Stern J, Mukamel R, Behnke E, Knowlton B, Fried I. Memory enhancement and deep-brain stimulation of the entorhinal area. *N Engl J Med.* 2012; 366(6):502–10.
  34. Laxton AW, Tang-Wai DF, McAndrews MP, Zumsteg D, Wennberg R, Keren R, Wherrett J, Naglie G, Hamani C, Smith GS, Lozano AM. A phase I trial of deep brain stimulation of memory circuits in Alzheimer's disease. *Ann Neurol.* 2010;68(4):521–34.